Physica D 306 (2015) 82–93

Contents lists available at ScienceDirect

Physica D

journal homepage: www.elsevier.com/locate/physd

Mobile localized solutions for an electron in lattices with dispersive and non-dispersive phonons

Luis A. Cisneros-Ake [a], Leonor Cruzeiro [b], Manuel G. Velarde [c,*]

[a] Department of Mathematics, ESFM, Instituto Politécnico Nacional, Unidad Profesional Adolfo López Mateos Edificio 9, 07738 México D.F., Mexico
[b] CCMAR and FCT, Universidade do Algarve, Campus de Gambelas, Faro-8005-139, Portugal
[c] Instituto Pluridisciplinar, Universidad Complutense de Madrid, Paseo Juan XXIII 1, Madrid-28040, Spain

HIGHLIGHTS

- An electron interacts both with on-site and with longitudinal phonons.
- We provide existence conditions for mobile localized electron excitations.
- We discuss discrete and continuum approaches to lattice dynamics.
- Localized states can be stable if they have a non-zero velocity.

ARTICLE INFO

Article history:
Received 30 September 2014
Received in revised form
18 May 2015
Accepted 19 May 2015
Available online 27 May 2015
Communicated by A. Mikhailov

Keywords:
Mobile localized states
Non-dispersive phonons
Dispersive phonons
Coupled phonon modes

ABSTRACT

We consider a one dimensional lattice in which an electron can interact both with on-site non-dispersive (Einstein) phonons and with longitudinal dispersive acoustic (Debye) phonons. We provide existence conditions for mobile localized electron excitations in the long wave limit. The role of both types of phonon modes on localization is also assessed, together with a discussion of differences existing between the discrete and the continuum approaches. A striking result is that, under certain conditions, localized states can only be stable if they have a non-zero velocity.

1. Introduction

In a crystal-lattice with harmonic interactions both dispersive (Debye) and non-dispersive (Einstein) phonons are expected to play a significant role in the material properties. The former (acoustic phonons) originates in the relative displacements of atoms while the latter demands consideration of just absolute atomic motions (so-called Einstein oscillators). The interaction of an electron with Debye and Einstein modes, separately, has been considered by Davydov [1] and Holstein [2,3]. Other studies have focused on the ground states of electrons in chains with the two types of phonon modes [4,5] and recently such chains have also been used to model thermal conductance in linear [6,7] and nonlinear [8] systems.

The system we are thinking about is that of a quasi-one dimensional chain embedded in a three dimensional structure. In this system, the dispersive (Debye) phonons describe the (longitudinal) interaction of the lattice sites within the one-dimensional structure and the non-dispersive (Einstein) phonons describe the interaction of each site in the one dimensional chain with the atoms or groups of atoms that surround the one dimensional chain. In a strict sense, the motion of the site in this one dimensional chain should be represented by a nonlinear potential, as the deviations from equilibrium positions, particularly in localized states, can be large when compared with the distance between sites. In fact, in previous studies, two of us have considered such cases [9–11]. However, a nonlinear lattice introduces the possibility of lattice solitons which, in turn, will tend to localize the electron states and makes it difficult to investigate the transition from localized to delocalized electron states. Furthermore, examples of systems whose bond vibrations are usually represented by harmonic potentials are proteins and DNA and other organic molecules for which the linear

* Corresponding author.
E-mail addresses: cisneros@esfm.ipn.mx (L.A. Cisneros-Ake), lhansson@ualg.pt (L. Cruzeiro), mgvelarde@pluri.ucm.es (M.G. Velarde).

http://dx.doi.org/10.1016/j.physd.2015.05.008
0167-2789/

frequencies used in potentials like GROMOS [12], or AMBER [13] or CHARMM [14] are those measured experimentally.

In [4] the best conditions for the existence of localized electron ground (i.e. stationary, non-moving) states were established. In particular, for discrete systems, it was found that these conditions were obtained when the electron–phonon interaction is dominated by non-dispersive phonons while the lattice energy is dominated by dispersive phonons. In such a case, the transition to a delocalized state, which in most cases always takes place above a threshold value of the electron exchange integral, can be completely suppressed. Here we extend the study to mobile, long wave limit solutions in a rather general framework embracing all possible excited states of the electron–phonon system.

In Section 2 we introduce the model Hamiltonian system we shall be considering, together with the corresponding evolution equations in a mixed quantum–classical approach. These equations contain four significant parameters that under appropriate approximations embrace the evolutionary problem treated in Ref. [4] as well as the so-called Davydov [1] and Holstein models [2,3]. Thus our model involves four significant tunable nonlinearities that can be reduced to just two by suitable change of scales. In order to proceed with as much as possible an analytical study, the discrete lattice problem is transformed into its natural long wave limit approximation in the continuum. We then obtain mobile solutions, that is, traveling wave solutions, and analyze their stability. In Section 3 we develop a variational Lagrangian approach to further characterize all possible solutions, mobile and otherwise, and discuss some significant limit cases. Section 4 deals with full numerical solutions specifying, for illustration purposes, particular albeit significant values of the parameters involved in the complete dynamics. Finally, we discuss how the mobile solutions anchor with the stationary results of Ref. [4] and what the differences are between the discrete and the continuum limit evolutionary problems. In Section 5 we provide some concluding remarks.

2. Model equations

We consider the Hamiltonian $\hat{H} = \hat{H}_{qp} + H_{ph} + \hat{H}_{qp-ph}$, where the first term describes the electron, the second term describes the lattice (with all sites being identical, with equal masses, M) and the third term describes the electron–lattice interactions. We take the lattice dynamics in the harmonic approximation and include both dispersive, Debye (D) phonons, and non-dispersive, Einstein (E) phonons. As usual a dot denotes time derivative. The three terms are thus as follows:

$$\hat{H}_{qp} = \sum_{n=-\infty}^{\infty} \left[\varepsilon_0 \hat{A}_n^{\dagger} \hat{A}_n - J \left(\hat{A}_n^{\dagger} \hat{A}_{n+1} + \hat{A}_{n+1}^{\dagger} \hat{A}_n \right) \right], \tag{1}$$

$$H_{ph} = \sum_{n=-\infty}^{\infty} \left[\frac{M}{2} \dot{q}_n^2 + \frac{\kappa_D}{2} (q_{n+1} - q_n)^2 + \frac{\kappa_E}{2} q_n^2 \right], \tag{2}$$

and

$$\hat{H}_{qp-ph} = \sum_{n=-\infty}^{\infty} \left[\chi_D \hat{A}_n^{\dagger} \hat{A}_n (q_n - q_{n-1}) + \chi_E \hat{A}_n^{\dagger} \hat{A}_n q_n \right], \tag{3}$$

where $\hat{A}_n^{\dagger}$ ($\hat{A}_n$) is the Fermi creation (annihilation) operator for an electron in site n, ε_0 is the energy of the electron, J is the transfer term for the electron to move from one site to its nearest neighbor, κ_D (κ_E) is the elasticity constant for Debye (Einstein) oscillators, q_n is the displacement from equilibrium positions of the lattice sites and χ_D (χ_E) is the strength of the electron interaction with the Debye (Einstein) phonons.

The general solution of $\hat{H}$, written in terms of a site basis set is $\psi = \sum_{n=-\infty}^{\infty} \psi_n \hat{A}_n^{\dagger} |0\rangle$, where $|0\rangle$ is the vacuum state and ψ_n depends on the lattice variables q_n, $\dot{q}_n$ and on the time t in a manner that is not specified *a priori*. From the appropriate variational principle, after a gauge transformation of the probability density function ψ_n to eliminate the on-site energy ε_0, we obtain the following equations of motion:

$$i\hbar \dot{\psi}_n = -J (\psi_{n-1} + \psi_{n+1}) + \chi_D (q_n - q_{n-1}) \psi_n + \chi_E q_n \psi_n, \tag{4}$$

and

$$M \ddot{q}_n = \kappa_D (q_{n-1} - 2q_n + q_{n+1}) - \kappa_E q_n + \chi_D \left(|\psi_{n+1}|^2 - |\psi_n|^2 \right) - \chi_E |\psi_n|^2 . \tag{5}$$

Re-scaling the variables in the form: $\rho_n = \frac{\kappa_D}{\chi_D} q_n$ and $\tau = \frac{J}{\hbar} t$ we get dimensionless equations of motion:

$$iV \dot{\psi}_n = -V (\psi_{n-1} + \psi_{n+1}) + \psi_n (\rho_n - \rho_{n-1}) + \chi \rho_n \psi_n, \tag{6}$$

$$m \ddot{\rho}_n = \rho_{n-1} - 2\rho_n + \rho_{n+1} - \kappa \rho_n + |\psi_{n+1}|^2 - |\psi_n|^2 - \chi |\psi_n|^2 , \tag{7}$$

where the time derivatives are now with respect to τ and

$$m = \frac{MJ^2}{\kappa_D \hbar^2}, \qquad \kappa = \frac{\kappa_E}{\kappa_D}, \qquad \chi = \frac{\chi_E}{\chi_D}, \qquad V = \frac{\kappa_D J}{\chi_D^2}. \tag{8}$$

Eqs. (6) and (7) interpolate between the Davydov [1] and Holstein [2,3] models, i.e. for $\kappa = 0$ and $\chi = 0$ we recover the Davydov model, whereas for $\kappa = \infty$ and $\chi = \infty$ the Holstein model is obtained. Setting $\kappa_D = \kappa_E = \kappa$ and $\chi_D = \chi_E = \chi$ leads to the regimes whose stationary states were investigated in [4].

In the continuum limit, at first order, Eqs. (6) and (7) reduce to

$$iV \psi_t = -V \psi_{xx} + \rho_x \psi + \chi \rho \psi, \tag{9}$$

$$m \rho_{tt} = \rho_{xx} - \kappa \rho + \left(|\psi|^2 \right)_x - \chi |\psi|^2 . \tag{10}$$

Our aim is to investigate the relative influence that dispersive (D) and non-dispersive (E) phonons have on the electron states and to determine the values of the parameters V, κ and χ that lead to the existence of localized *mobile* solutions. But to start with, we first explore, in a general way, the kind of traveling solutions that can be expected from Eqs. (9)–(10).

2.1. Traveling wave solutions

We look for traveling wave solutions of the coupled system (9)–(10) in the standard form:

$$\psi (x, t) = e^{i(rx - st)} f (x - ct) , \tag{11}$$

$$\rho (x, t) = g (x - ct) . \tag{12}$$

For the wave function ψ to be localized, f must decay to zero as $|z| = |x - ct| \to \infty$. We make no assumptions, at this moment, about the profile for the lattice distortion ρ, which, for some values of the parameters κ and χ is a pulse but for other values, locally, can even be a kink.

In the traveling reference frame for the system of Eqs. (9)–(10), we have

$$Vf'' + iV (2r - c) f' + V \left(s - r^2 \right) f = fg' + \chi fg, \tag{13}$$

$$\left(mc^2 - 1 \right) g'' = -\kappa g + \left(f^2 \right)' - \chi f^2, \tag{14}$$

where the prime denotes differentiation with respect to the traveling coordinate $z = x - ct$. We now take the values $c = 2r$ and $\beta = r^2 - s = \frac{c^2}{4} - s$ and define the parameters $\overline{\kappa}^2 = \kappa / \left(1 - mc^2 \right)$ and $\gamma = 1 / \left(1 - mc^2 \right)$ thus leading to

$$Vf'' = f \left[V\beta + g' + \chi g \right], \tag{15}$$

$$0 = g'' - \overline{\kappa}^2 g + \gamma \left[\left(f^2 \right)' - \chi f^2 \right]. \tag{16}$$

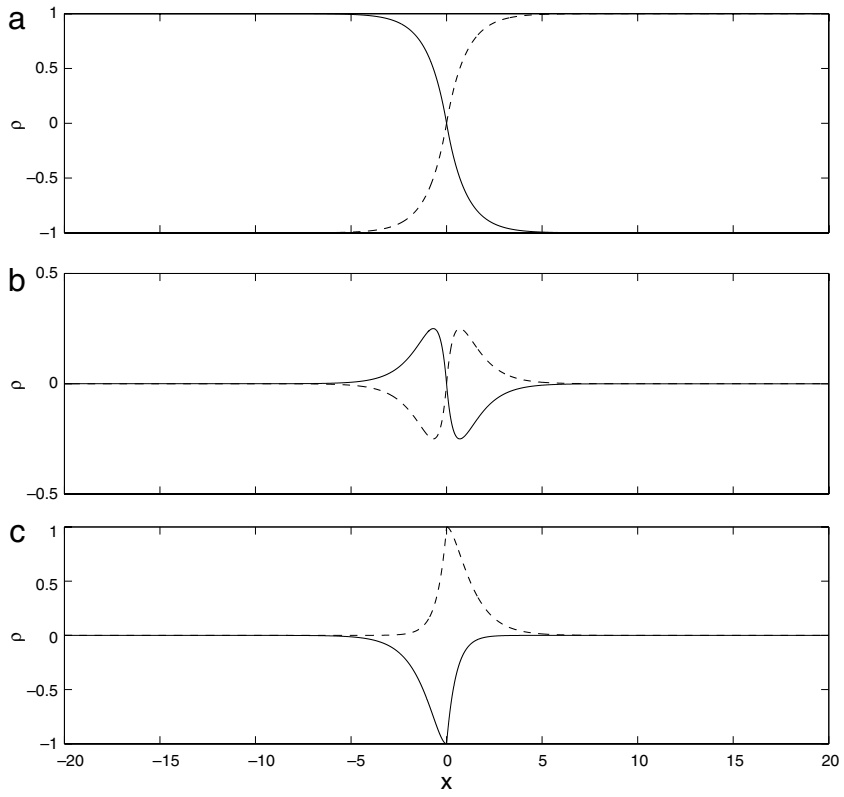

Fig. 1. Typical profiles of the lattice distortion, ρ. (a) Solid line: $\beta = 0, C = 0, \gamma = 1, B = 1$ (dashed line: $B = -1$). (b) Solid line: $\beta = 2, C = 0, \gamma = 1, B = -1$ (dashed line: $B = -2, C = -1$). (c) Solid line: $\beta = 2, C = -1, \gamma = 1, B = 1$ (dashed line: $B = 1, C = 1$).

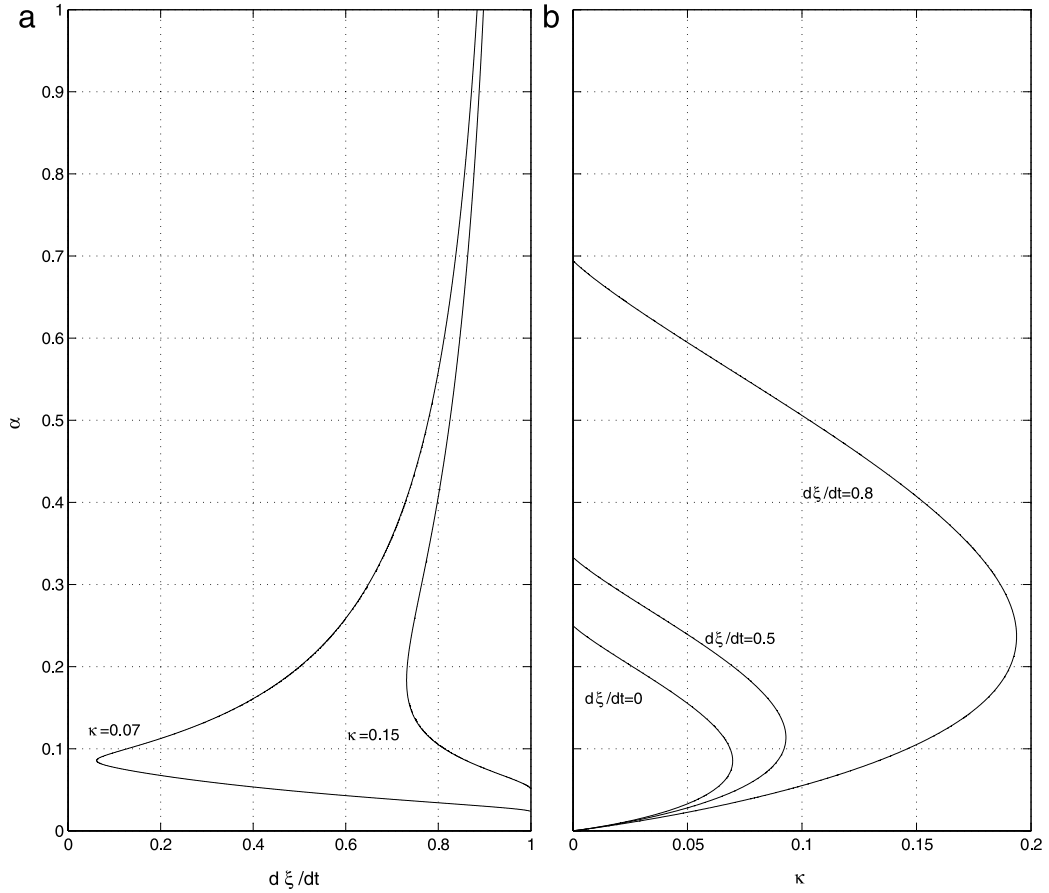

Fig. 2. Dispersion relation: (a) $\alpha = \alpha(\dot{\xi})$ for two values of κ, and (b) $\alpha = \alpha(\kappa)$ for three values of $\dot{\xi}$. All curves are obtained from (29) and (31) with $V = 0.5$ and $m = 1$.

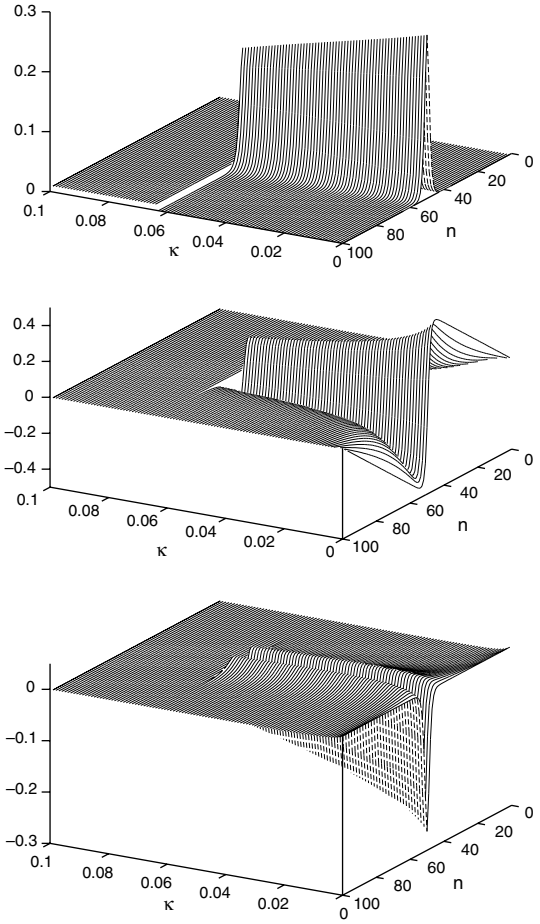

Fig. 3. Numerically energy minimized states for an electron in a lattice with 100 sites. Top plot is the electron probability in site n, $|\psi_n|^2$, middle plot is the lattice displacements, ρ_n and bottom plot is relative lattice displacements, $\rho_n - \rho_{n-1}$. $V = 0.5$, $\chi = 0$ (electron–lattice interaction dominated by dispersive Debye modes) and κ varies (right to left) from 0 (Davydov case) to 0.1 thus accounting for the role of on-site Einstein modes.

Then Eq. (16) can be solved for g by means of the Fourier Transform in the traveling coordinate z. Doing this, in the Fourier space we obtain:

$$0 = -w^2\hat{g} - \bar{\kappa}^2\hat{g} - iw\gamma\hat{f^2} - \gamma\chi\hat{f^2}, \tag{17}$$

where $\hat{g} = \mathcal{F}\{g\}$ is the Fourier Transform of g. Let $F(w) = \hat{f^2} = \mathcal{F}\left\{f^2\right\}$, then Eq. (17) simplifies to

$$\hat{g} = -i\gamma\frac{w}{w^2+\bar{\kappa}^2}F(w) - \gamma\chi\frac{1}{w^2+\bar{\kappa}^2}F(w). \tag{18}$$

We finally use the convolution property of the Fourier Transform and the Heaviside function to solve for g in the form:

$$g(z) = \frac{\gamma}{2}\int_0^\infty e^{-\bar{\kappa}\xi}\left[f^2(z+\xi) - f^2(z-\xi)\right]d\xi - \frac{\gamma\chi}{2\bar{\kappa}}\int_0^\infty e^{-\bar{\kappa}\xi}\left[f^2(z+\xi) + f^2(z-\xi)\right]d\xi. \tag{19}$$

Since $f = |\psi|$ is the probability density wave function for an electron, it has to be bell shape type. On the other hand, it is easy to see that the integral expression for g in Eq. (19), in general, is not simplified in terms of elementary functions, for all decaying function f. In order to obtain analytical expressions, we set $f = Ae^{-\alpha|x-\xi(t)|}$ and find, after a straightforward integration, that the profile for g can be described by the following combination of exponentials:

$$\rho(x,t) = \begin{cases} B\left[e^{-\gamma(x-\xi(t))} - e^{-\beta(x-\xi(t))}\right] + Ce^{-\gamma(x-\xi(t))}, & x > \xi(t) \\ B\left[e^{\beta(x-\xi(t))} - e^{\gamma(x-\xi(t))}\right] + Ce^{\gamma(x-\xi(t))}, & x \le \xi(t) \end{cases} \tag{20}$$

where the wave parameters B, C, γ and β clearly depend on the model parameters V, κ and χ and the parameters describing the electron wave function A and α. Varying the wave parameters we find that, according to (20), the lattice distortion ρ can only assume one of the three shapes displayed in Fig. 1, i.e. the exponential wave profiles given by (20) can be either a pulse with one hump, a flip-flop or a kink. In particular, the kink profile of Fig. 1(a) is obtained for $\beta = 0$ and $C = 0$ and corresponds to the lattice solution in the Davydov limit ($\kappa = \chi = 0$) [15]. The expressions for the wave parameters in (20) will be derived in the next section using a variational approach.

3. Variational approach

The variational approach developed in this section is standard and based on the modulation theory of Whitham [16] according to which the Lagrangian associated with the equations of motion is averaged over an appropriate family of trial functions. The equations of motion (9)–(10) can be derived from the Lagrangian:

$$L = \int_{-\infty}^{\infty}\left[\frac{m}{2}\rho_t^2 - \frac{1}{2}\rho_x^2 - \frac{\kappa}{2}\rho^2 + \frac{iV}{2}\left(\psi_t\psi^* - \psi_t^*\psi\right) - V|\psi_x|^2 - \rho_x|\psi|^2 - \chi\rho|\psi|^2\right]dx. \tag{21}$$

In order to select appropriate trial functions we use the results of the previous section according to which an exponential decay in the probability density wave function $|\psi(x,t)|$ implies either an exponential decay or a constant value at the tails of the lattice distortion $\rho(x,t)$, depending on the values of the parameters V, κ and χ. Furthermore, to obtain analytically manageable expressions for the integrals of interaction, when averaging the Lagrangian (21), we set:

$$\psi(x,t) = Ae^{-\alpha|x-\xi(t)|}e^{i[\phi(t)+v(t)(x-\xi(t))]}, \tag{22}$$

and, for the lattice profile $\rho(x,t)$, the combination of exponentials expressed in Eq. (20).

Averaging the Lagrangian (21) on the family of profiles (20) and (22) we obtain:

$$L = \frac{m\dot{\xi}^2 - 1}{2}\frac{B^2(\beta-\gamma)^2 + C^2\gamma(\beta+\gamma)}{\beta+\gamma} - \frac{\kappa}{2}\frac{B^2(\beta-\gamma)^2 + C^2\beta(\beta+\gamma)}{\beta\gamma(\beta+\gamma)} - \frac{4A^2B\alpha(\beta-\gamma)}{(2\alpha+\beta)(2\alpha+\gamma)} - \frac{2\chi A^2C}{2\alpha+\gamma} - A^2\left(\dot{\phi} - v\dot{\xi}\right)\frac{V}{\alpha} - A^2\left(\alpha^2+v^2\right)\frac{V}{\alpha}, \tag{23}$$

where $\dot{\xi} =$ constant and $\dot{\phi} =$ constant provide stationary traveling waves. The variational principle permits to obtain relationships between the variational parameters α, β, γ, B, C, A and the physical parameters of the original system m, κ, χ and V as it is shown below.

Variation of the averaged Lagrangian (23) in the wave parameters B and C gives,

$$B = \frac{4A^2\alpha\beta\gamma(\beta+\gamma)}{(2\alpha+\beta)(\beta-\gamma)(2\alpha+\gamma)\left[\left(-1+m\dot{\xi}^2\right)\beta\gamma - \kappa\right]}, \tag{24}$$

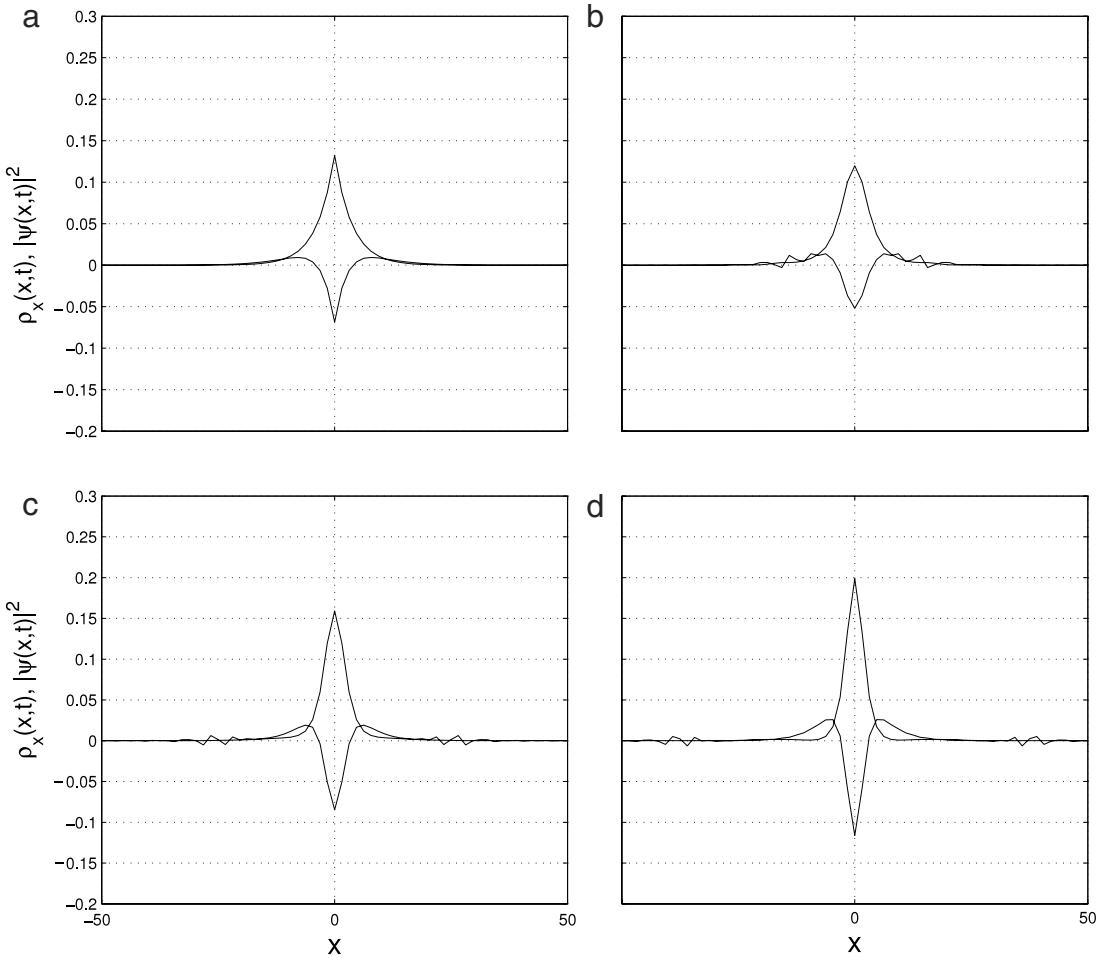

Fig. 4. Lattice distortion, $\rho_x(x,t)$, pointing downwards and electron probability density, $|\psi(x,t)|^2$, pointing upwards. Full numerical solution of the continuum system (9)–(10) for $V = 0.5$, $\kappa = 0.06$, $\chi = 0$, $m = 1$, with a stationary profile given by (20) and (22), with $\dot{\xi} = 0$, $\alpha = 0.132$, at (a) $t = 0$, (b) $t = 12.26$, (c) $t = 24.47$ and (d) $t = 36.68$.

and

$$C = \frac{2A^2\gamma\chi}{(2\alpha+\gamma)\left[\left(-1+m\dot{\xi}^2\right)\gamma^2-\kappa\right]}, \tag{25}$$

respectively. These two expressions provide the dependence of the amplitude of the lattice distortion $\rho(x,t)$ as a function of κ and χ. We should also note that both B (24) and C (25) are proportional to the amplitude A of $|\psi|$, as expected in the polaron theory where the electron creates a lattice deformation which traps the electron itself [1,15]. As a side remark it is noteworthy that in some anharmonic lattices, longitudinal distortions in the form of acoustic solitons, traveling supersonically, not only trap the electron but also are able to drag it, thus generalizing the polaron concept [9–11].

Taking the variation in the wave parameter β and using expression (24) for B we find a relation for the parameter γ in the form:

$$\gamma = \frac{(2\alpha-\beta)\left[\beta^2\left(1-m\dot{\xi}^2\right)+\kappa\right]+\sqrt{\Delta}}{4\beta^2\left(1-m\dot{\xi}^2\right)}, \tag{26}$$

where the positive root yields positive values of γ and

$$\Delta = (2\alpha-\beta)^2\left[\beta^2\left(1-m\dot{\xi}^2\right)+\kappa\right]^2+32\beta^3\alpha\kappa\left(1-m\dot{\xi}^2\right).$$

On the other hand, taking the variation in γ and using Eqs. (24)–(25) for B and C we get the dispersion relation:

$$\chi^2 = \frac{4\alpha^2\beta\left[\left(1-m\dot{\xi}^2\right)\gamma^2+\kappa\right]^2 h_1}{(2\alpha+\beta)^2\left[\beta\gamma\left(1-m\dot{\xi}^2\right)+\kappa\right]^2}, \tag{27}$$

where

$$h_1 = \frac{\left(1-m\dot{\xi}^2\right)\beta\gamma^2(2\beta+\gamma-2\alpha)+\beta\gamma\kappa-2\alpha\kappa(2\gamma+\beta)}{\gamma^2(3\gamma+2\alpha)\left(-1+m\dot{\xi}^2\right)-\gamma\kappa+2\alpha\kappa}.$$

Combining the variations in A and α and using again the expressions for B and C we get another dispersion relation in the form:

$$\chi^2 = \frac{\alpha(2\alpha+\gamma)\left[\left(-1+m\dot{\xi}^2\right)\gamma^2-\kappa\right]h_2}{2A^2(2\alpha+\beta)^3\gamma^2}, \tag{28}$$

where

$$h_2 = \frac{16A^2\alpha\beta\gamma(\beta+\gamma)(\beta\gamma+\alpha(\beta+\gamma))}{(2\alpha+\gamma)\left(\left(1-m\dot{\xi}^2\right)\beta\gamma+\kappa\right)} - V(2\alpha+\beta)^3(2\alpha+\gamma)^2.$$

Finally, variation in v gives $\dot{\xi} = 2v$ while the normalization condition $\int_{-\infty}^{\infty}|\psi(x,t)|^2\,dx = 1$ for the probability density $|\psi|^2$ leads to $A^2 = \alpha$.

We thus conclude that the trial functions (20) and (22), together with the wave parameters obtained from the dispersion relations (24)–(28) for arbitrary velocity v and normalized amplitude A, lead to a two-parameter family of approximate solutions to the full continuum system (9)–(10) for any values of the model parameters m, V, χ and κ. Conversely, the values of A and v for the electron probability density $|\psi|^2$ (22) in the moving frame determine the

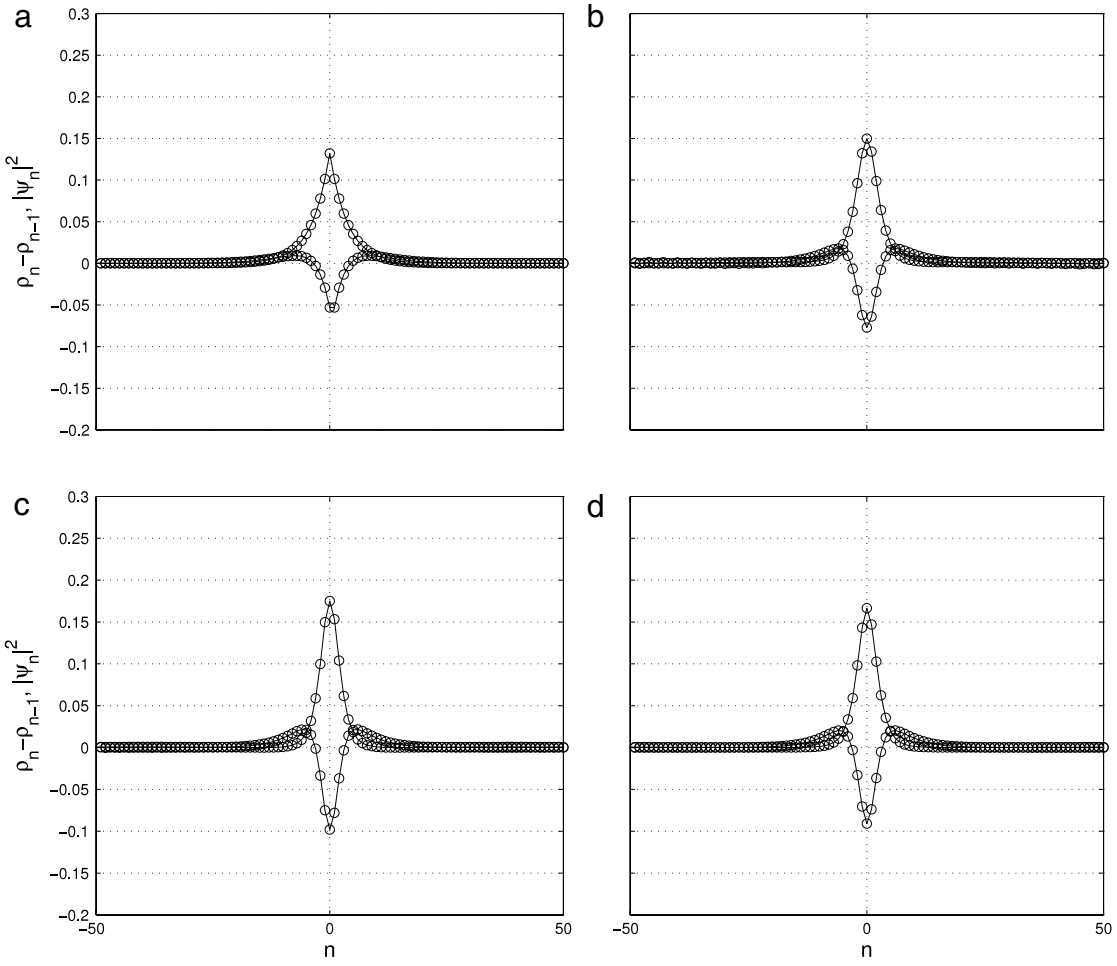

Fig. 5. Lattice distortion, $\rho_n - \rho_{n-1}$, pointing downwards and electron probability density, $|\psi_n|^2$, pointing upwards. Full numerical solution of discrete system (6)–(7) at (a) $t = 0$, (b) $t = 80$, (c) $t = 160$ and (d) $t = 240$. The parameters for the system and the initial condition are the same as for the continuum model in Fig. 4.

wave parameters for the lattice distortion $\rho(x, t)$ in agreement with polaron theory.

As a starting point of the analysis of the dispersion relations (24)–(28) we first notice that (26)–(28) only involve the wave parameters γ, β, α, $\dot{\xi}$ and A in terms of the model lattice parameters in Eqs. (6)–(7) as expected. Setting $v = \dot{\xi}/2$ and $A = \sqrt{\alpha}$ into expressions (26)–(28) and substituting (26) in (27) and (28) we get two independent nonlinear implicit algebraic equations involving the wave parameter β and the lattice parameters m, V, κ and χ. Furthermore, we can eliminate χ from those two implicit relations which leads to a single implicit algebraic equation that only depends on β, κ, V and m. We then obtain β in terms of κ, V and m for given wave parameters $\dot{\xi}$ and α and the rest of the wave parameters are obtained in this manner: first, γ is derived from Eq. (26) and, secondly, B and C are deduced from Eqs. (24) and (25).

In order to gain further insight into the transition from localized to delocalized states we will consider two limit cases in the next subsections.

3.1. Case study: $\chi = 0$

The first limit case we consider is that in which the lattice dynamics includes both dispersive ($\kappa_D \neq 0$) and non-dispersive ($\kappa_E \neq 0$) phonons while the electron–lattice interactions are dominated by Debye dispersive modes ($\chi_D \gg \chi_E$). From Eqs. (27) and (28) it follows that $\chi = 0$ if $\gamma = 2\alpha$. Thus Eq. (25) reduces to $C = 0$ and Eq. (26) to:

$$\dot{\xi} = \frac{1}{\sqrt{m}}\sqrt{1 - \frac{\kappa}{\beta^2}}. \tag{29}$$

Since κ and β are both positive Eq. (29) limits solutions to subsonic waves (sound velocity is $\frac{1}{\sqrt{m}}$). Introducing expression (29) for $\dot{\xi}$ into Eq. (24) yields:

$$B = \frac{2\alpha^2\beta^2}{\kappa\left(4\alpha^2 - \beta^2\right)}. \tag{30}$$

Also, combining (27) and (28) leads to:

$$\kappa = \frac{\alpha\beta^2\left(2\alpha + 3\beta\right)}{2V\left(2\alpha + \beta\right)^3}, \tag{31}$$

thus providing an implicit (nonlinear) dispersion relation between the wave parameters α and β for given κ. The dispersion relation $\alpha = \alpha(\dot{\xi})$ obtained from the combination of (29) and (31) for $V = 0.5$ and $m = 1$ is displayed in Fig. 2(a) for two fixed values of κ. We should note that α close to 1 corresponds to strong localized solutions, while α close to zero corresponds to delocalized solutions. Fig. 2 illustrates a very striking result, namely, that *above a critical value of κ, localized solutions exist only if the velocity $\dot{\xi}$ is finite*. As κ increases, the lower velocity, corresponding to the turning point in the branch of solutions, tends to the sound velocity, $1/\sqrt{m}$. It is also apparent from Fig. 2(a) that for a given

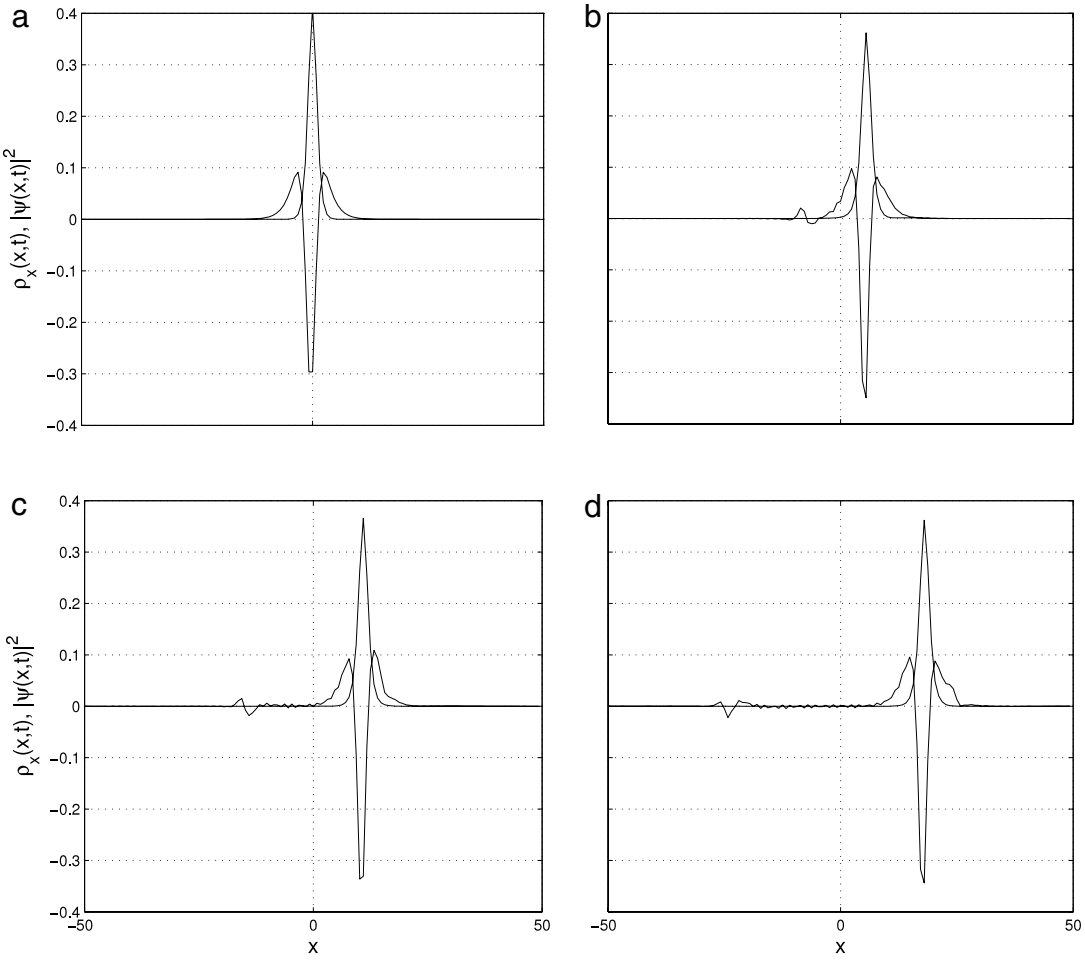

Fig. 6. Lattice distortion, $\rho_x(x,t)$, pointing downwards and electron probability density, $|\psi(x,t)|^2$, pointing upwards. Full numerical solution of the continuum system (9)–(10) with moving profile given by (20) and (22), with $\dot{\xi} = 0.8$, $\alpha = 0.41$, at (a) $t = 0$, (b) $t = 7.56$, (c) $t = 14.89$ and (d) $t = 24.65$. The parameters for the system are the same as in Fig. 4, except that $\kappa = 0.15$.

κ, say $\kappa = 0.07$, thin or strongly localized (α close to 1) mobile polarons travel faster than wide or strongly delocalized (α close to 0) mobile polarons, as it is generally found in soliton theory.

Let us determine the critical value κ^* above which only mobile localized solutions exist by considering the stationary state, $\dot{\xi} = 0$, together with Eq. (29), which leads to $\beta = \sqrt{\kappa}$ which, in turn, reduces (31) to:

$$\frac{\alpha\,(2\alpha + 3\beta)}{2V\,(2\alpha + \beta)^3} = 1. \tag{32}$$

The latter equation provides α as a function of κ for $V = 0.5$ and is depicted in the curve $\dot{\xi} = 0$ of Fig. 2(b). This curve shows that there is a turning point at approximately $\kappa^* = 0.0698$, for $V = 0.5$. It also shows that, for $\kappa = 0$, there are *two* possible values of α: $\alpha = 0$, which corresponds to a completely delocalized electron state and $\alpha = \frac{1}{8V} = 0.25$, which corresponds to a localized state. $\chi = 0$, $\kappa = 0$ correspond to the cases studied by Davydov [1] who showed that any finite electron–lattice interaction leads to a localized, soliton solution. Thus, $\alpha = \frac{1}{8V} = 0.25$ corresponds exactly to Davydov's solution. Indeed, for the set of Eqs. (29)–(31) the trial function (20) for $\rho\,(x,t)$ reduces to the solid curve shown in Fig. 1(b) and, in particular, to the solid curve of Fig. 1(a) for $\kappa = 0$. We then recover the kink profile of Fig. 1(a) from Fig. 1(b) when we satisfy (31) for $\kappa = 0$, that is, when $\beta = 0$. In this case:

$$\lim_{(\kappa,\beta)\to(0,0)} \frac{\kappa}{\beta^2} = \frac{1}{8V\alpha}, \tag{33}$$

and hence Eq. (29) becomes

$$\dot{\xi} = \frac{1}{\sqrt{m}}\sqrt{1 - \frac{1}{8V\alpha}}, \tag{34}$$

where, to have real values for the velocities, we must impose $8V\alpha \geq 1$. We also get $B = 4V\alpha$ which recovers Davydov's kink profile for the lattice function $\rho\,(x,t)$ in the continuum limit [1].

Since we recover the Davydov limit for $\kappa = 0$ and $\alpha = \frac{1}{8V}$, then the upper branch of the $\dot{\xi} = 0$ curve in Fig. 2(b) is the continuation in κ of the stationary normalized Davydov soliton. On the other hand, the connecting lower branch, which leads to the completely delocalized solution for $\kappa = 0$ corresponds to a higher energy state. We must emphasize that Fig. 2(b) is not a bifurcation diagram but a picture of how a normalized Davydov soliton can evolve, in the presence of non-dispersive phonons, to a completely delocalized solution.

The curves in Fig. 2(b) provide even more clear evidence for the fact that, when κ increases above κ^* the polaron must move in order to exist, i.e., above κ^* only traveling polarons are stable. Moreover, *as $\dot{\xi}$ increases from zero, the corresponding critical value κ^*, at the turning point, also increases*. While for small values of κ there are localized traveling solutions with any velocity, for larger values of κ beyond κ^* traveling solutions with lower velocities cannot exist. For example, for $\kappa > 0.1$ a localized traveling solution is not stable if the velocity $\dot{\xi}$ is equal to 0.5 but it becomes stable if the velocity is 0.8.

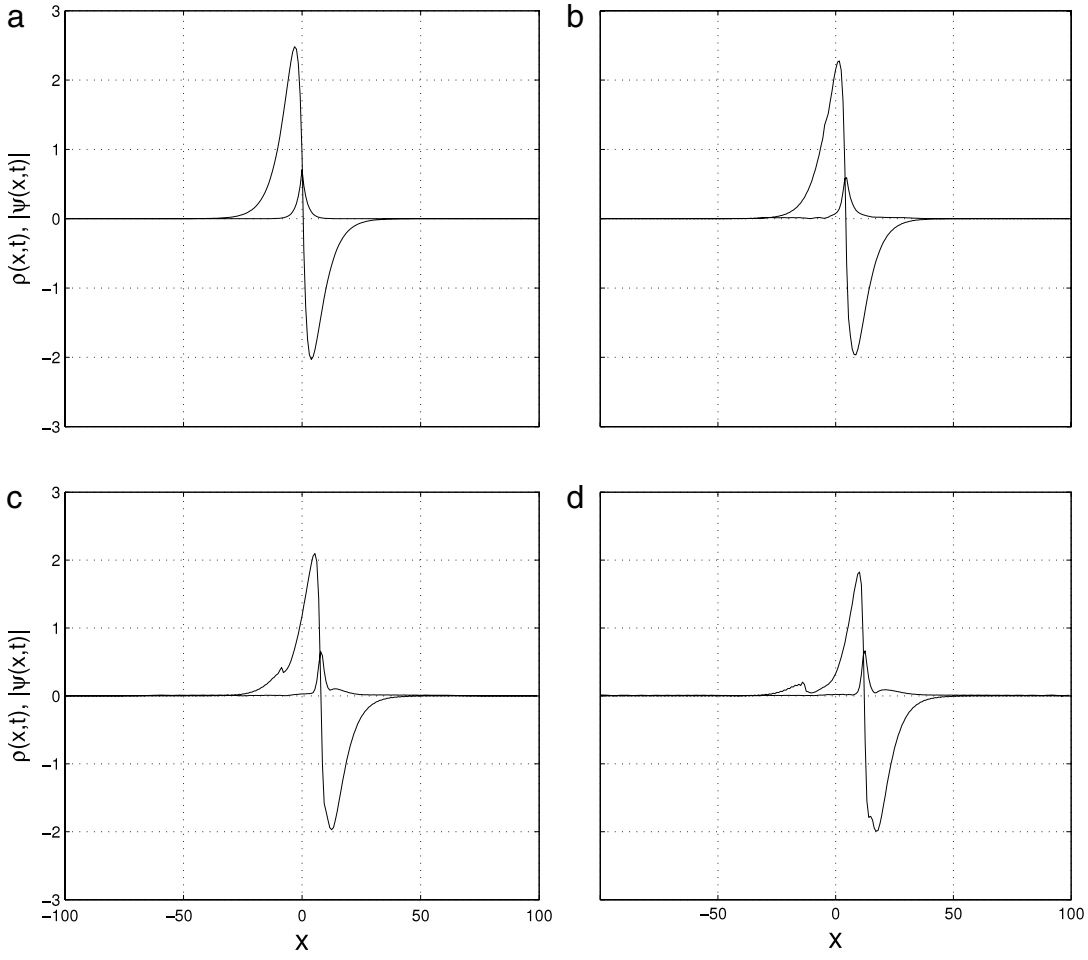

Fig. 7. Lattice displacement, $\rho(x,t)$, pointing downwards and absolute electron probability amplitude, $|\psi(x,t)|$, pointing upwards. Full numerical solution of the continuum system (9)–(10) for $V=1, \kappa=0, \chi=0.1, m=1$, and initial profile given by (20) and (22), with $\alpha=0.5, \gamma=0.4, \beta=2(\alpha-\gamma)$, at (a) $t=0$, (b) $t=4.3945$, (c) $t=8.667$ and (d) $t=13.5498$.

On the other hand, we observe from Eq. (29) that in the sonic limit, $\dot{\xi}=\frac{1}{\sqrt{m}}$, β tends to infinity which in turn gives the asymptotic limit of (31) as $\alpha=\frac{2V\kappa}{3}$. Since the normalization condition has to be satisfied, we may also conclude that for any finite velocity $0\leq\kappa\leq\frac{3}{2V}$. Thus for $V=0.5$ the maximum allowed value of κ, in principle, is $\kappa=3$, for almost sonic velocities. However, this is actually not the case since near the sonic limit the branches shown in Fig. 2(b) are basically straight lines $\alpha=\frac{2V\kappa}{3}$, with no turning point. Therefore, typical finite velocities and their corresponding allowed κ's are those displayed in Fig. 2(b).

We have confirmed that the analytical results given by (29)–(32) are also valid for the original full discrete lattice, described by Eqs. (6) and (7). Thus, setting $\chi=0$ (electron–lattice interaction dominated by dispersive Debye phonons) and $V=0.5$ we have determined numerically the minimum energy states, using periodic boundary conditions, varying from $\kappa=0$ to $\kappa=0.1$. The results are displayed in Fig. 3. We see that for $\kappa<0.063$ there are localized minimum energy states, but above that value the ground states of the electron are delocalized and associated with zero distortions in the lattice. The transition from localized to delocalized states is abrupt, as found in [4]. The value at which this transition takes place is very close to that of the analytical solution, i.e. the continuum limit approach (9)–(10) gives a good approximation to the original discrete system (6)–(7), at least for the stationary state. The continuation here by minimization corresponds to the upper branch of Fig. 2(b) for $\dot{\xi}=0$.

3.2. Case study: $\kappa=0$

We now consider the situation where the lattice system only includes dispersive phonons ($\kappa_E=0, \kappa_D\neq0$) and the Einstein modes dominate over the Debye modes in the electron–phonon interaction ($\chi_E\gg\chi_D$). From the combination of Eqs. (27) and (28) it follows that $\kappa=0$ when $\beta=2(\alpha-\gamma)$ for $0\leq\gamma\leq\alpha$ which in turn reduces Eq. (27) to

$$\chi^2=-\frac{\alpha^2(2\alpha-3\gamma)\gamma^2}{(\gamma-2\alpha)^2(2\alpha+3\gamma)}, \tag{35}$$

from which we derive the domain condition on γ: $\frac{2\alpha}{3}\leq\gamma\leq\alpha$. Combining Eqs. (28) and (35) yields

$$\dot{\xi}=\frac{1}{\sqrt{m}}\sqrt{1-\frac{2\alpha^2\left(2\alpha^2+3\alpha\gamma-3\gamma^2\right)}{(2\alpha+3\gamma)\left(\gamma^2-4\alpha^2\right)^2V}}, \tag{36}$$

where once again the normalization condition $A^2=\alpha$ has been used. Also Eqs. (24) and (25) for the amplitude expressions B and C of the lattice distortion reduce to

$$B=-\frac{(\gamma-2\alpha)^2(\gamma+2\alpha)(2\alpha+3\gamma)V}{4\alpha^3-15\alpha\gamma^2+9\gamma^3}, \tag{37}$$

$$C=-\frac{\left(\gamma^2-4\alpha^2\right)\sqrt{9\gamma^2-4\alpha^2}V}{2\alpha^2+3\alpha\gamma-3\gamma^2}. \tag{38}$$

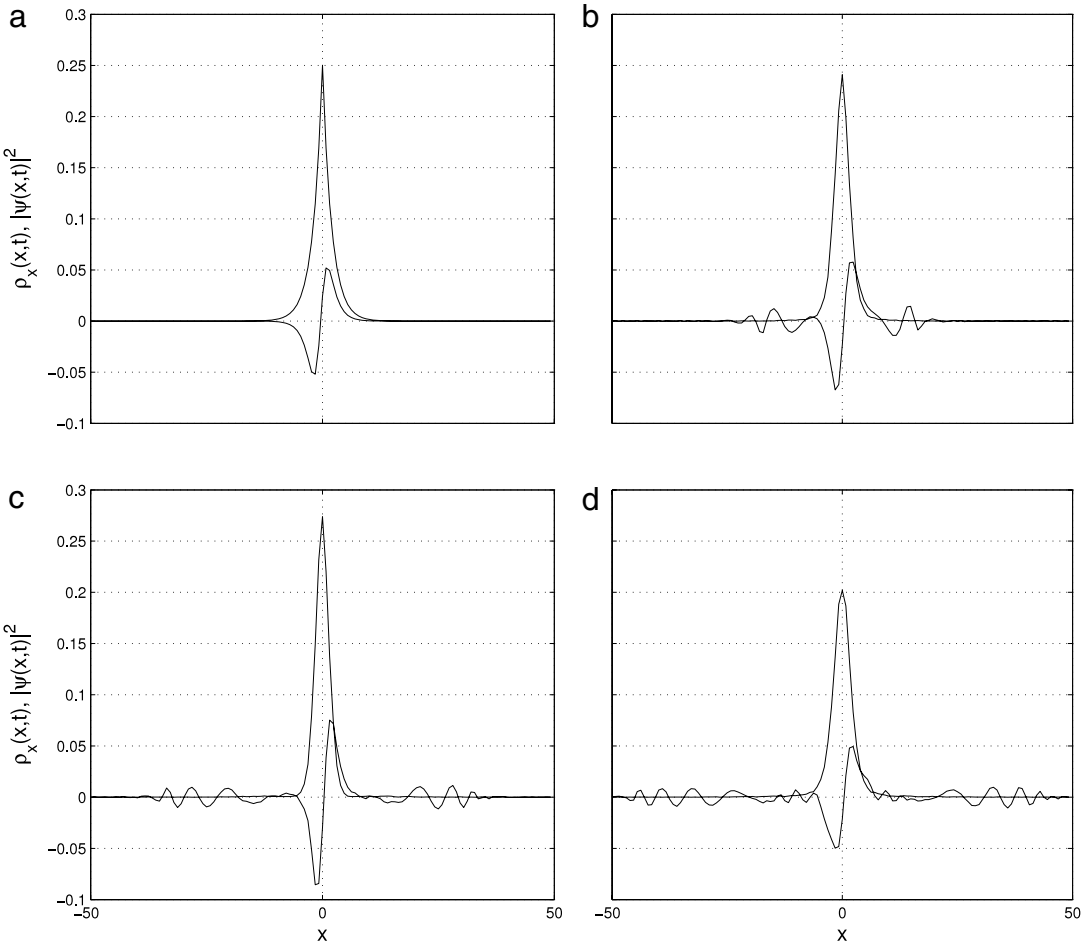

Fig. 8. Lattice distortion, $\rho_x(x,t)$, pointing downwards and electron probability density, $|\psi(x,t)|^2$, pointing upwards. Full numerical solution of the continuum system (9)–(10) for $V = 0.5$, $\kappa = 1$, $\chi = 1$, $m = 1$, with a stationary profile given by (20) and (22), with $\alpha = 0.25$, $\dot{\xi} = 0$, $\gamma = 0.3361$, $\beta = 1.4403$, $C = -0.1878$ and $B = -0.0809$, at (a) $t = 0$, (b) $t = 18.31$, (c) $t = 36.62$ and (d) $t = 48.82$.

We thus have again a two parameter family of solutions, which is further restricted by Eq. (35).

In the next section we check, by numerical means, the analytical predictions obtained in this section.

4. Full numerical solutions

To complete our study and indeed to cross-check the results obtained so far, in this section we compare them with results obtained from the numerical integration of the discrete (cf. Eqs. (6)–(7)) and of the continuum (cf. Eqs. (9)–(10)) systems. The continuum system is solved by the Pseudo Spectral Method (PSM) in space [17] and the ordinary differential equations derived with the PSM are integrated using a fourth-order Runge–Kutta method. Also, we make use of the wave parameters obtained from the variational approach developed in the previous section, in the wave profiles (20)–(22), to set appropriate initial conditions for the numerical integrations. Finally, the values of the parameters of the system are selected to test the stability of the corresponding solutions obtained by the variational approach.

For illustrative purposes, we start our numerical analysis by considering our findings in the limit case of section 3.1. To this end we take $m = 1$, $\chi = 0$, $\kappa = 0.06$ and $V = 0.5$ in the stationary state of the model equations (9)–(10) with initial conditions taken from the waves profiles (20)–(22) for $\rho(x,t)$ and $\psi(x,t)$, with free wave parameters $\alpha = 0.132$ and $\dot{\xi} = 0$, corresponding to Davydov's upper branch of Fig. 2(b). We display in Fig. 4 the numerical evolution of this stationary solution in the continuum lattice. The lattice function $\rho(x,t)$ has a flip-flop shape that recovers, in the Davydov limit of $\kappa = \chi = 0$, the anti-kink form corresponding to the Davydov soliton. Furthermore, we notice that for these parameter values, the widths of both the electron state and the lattice displacement profile are very similar. Fig. 4 also shows that the compression $\rho_x(x,t)$ has a minimum where the probability density function $|\psi(x,t)|^2$ attains its maximum. In this way, the lattice distortion $\rho_x(x,t)$ acts as a potential well for the electron, as expected with acoustic phonons. We also note that the initial spiky wave function for the electron evolves into a more bell- or sech-shaped form, as a little radiation leaks out, while the lattice profile remains largely unaltered, thus demonstrating the degree of stability of the initial condition (the lattice wave that travels in the backwards direction is due to the adjustment of the spiky initial envelope to the more exact solution and to conservation of global momentum).

To confirm that the stationary soliton is also stable in the discrete system, we consider the same parameter conditions and profiles but now as initial conditions for (6)–(7). Fig. 5 shows that the wave profiles obtained in the variational approach are indeed stable in the corresponding discrete system. In fact, as comparison of Figs. 4 and 5 demonstrates, the numerical evolution of the spiky initial conditions is actually better in the discrete case than in the continuum case. This is because the PSM is designed to smooth the solutions, which makes the peak profiles obtained from our variational approximation, poor initial conditions for the integration of the continuum system (9)–(10), and leads to the emission of linear radiation and slight variations in the amplitudes

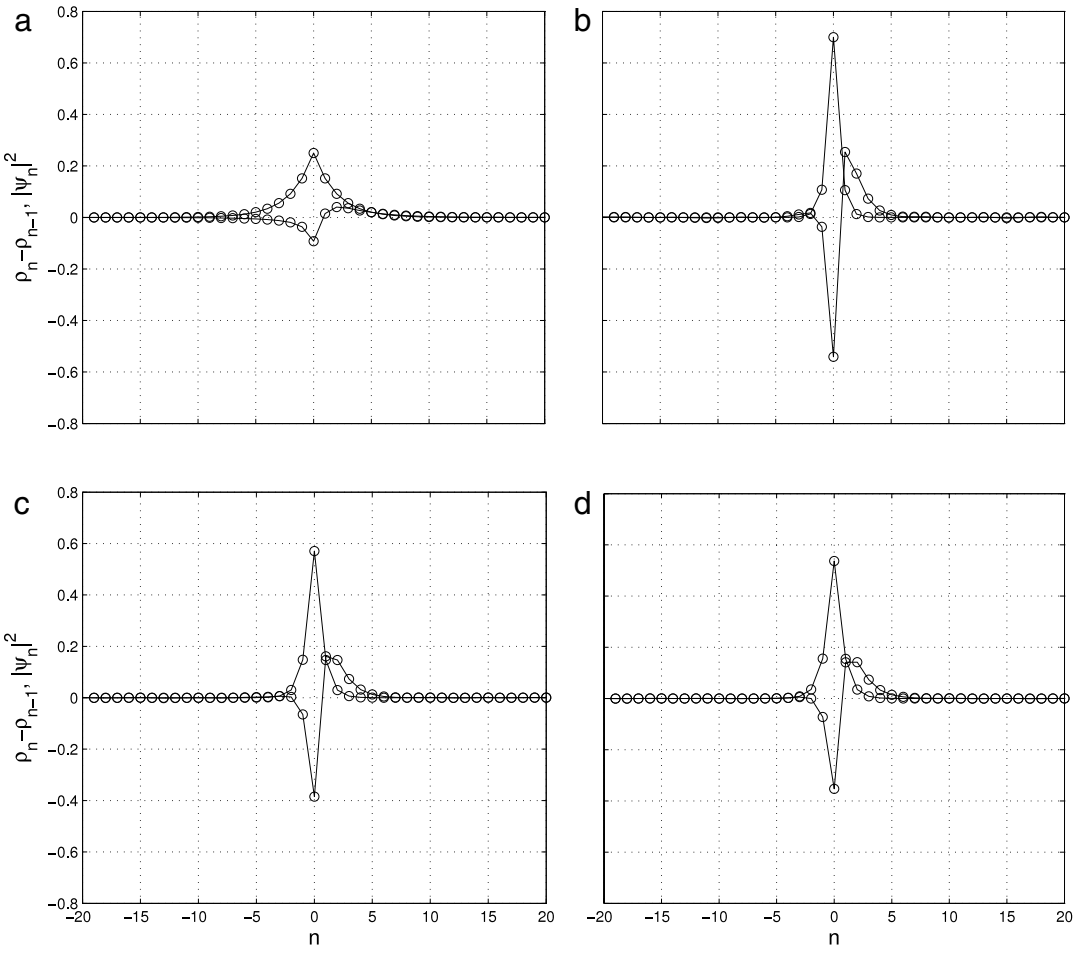

Fig. 9. Lattice distortion, $\rho_n - \rho_{n-1}$, pointing downwards and electron probability density, $|\psi_n|^2$, pointing upwards. Full numerical solution of discrete system (6)–(7) at (a) $t = 0$, (b) $t = 100$, (c) $t = 200$ and (d) $t = 300$. The parameters for the system and the initial condition are the same as for the continuum model in Fig. 8.

of the waves. Between Fig. 5(a) and (b) there is a transient in the solutions in the form of emission of linear waves that helps to adjust the initial conditions to the exact numerical ones.

To further test the stability of our numerical solutions, we consider also evolutions in the moving frame. We thus picked parameter values from Fig. 2(b) for the case $\dot{\xi} = 0.8$ and $\alpha = 0.41$. Fig. 6 shows the corresponding evolution in the continuum model until $t = 24.65$. We observe that the waves remain coherent as they move forward, with only a small change to the core of the lattice profile ρ, due to the PSM approximation.

Finally, to complete our analysis of the case study 3.1, we have verified that when initial conditions are taken from the lower branch of Fig. 2(b), in the stationary state, they evolve to the corresponding solution in the upper branch, for both the continuum (9)–(10) and the discrete (6)–(7) model equations (not shown). This demonstrates the instability of the solutions in the lower branch as well as the stability of the solutions in the upper branch.

Let us now consider the situation studied in Section 3.2. Fig. 7 shows the full numerical solutions for the case $\kappa = 0$ and $\chi = 0.1$. The wave parameters needed in the wave profiles (20)–(22) are obtained from the (nonlinear) dispersion relations (35), (36) and (38). In this case the lattice distortion $\rho(x, t)$ also has a flip-flop shape in the core region, in agreement with the Davydov limit for which the anti-kink form has to be recovered. For these parameter values, the width of the lattice distortion profile is larger than the width of the electron probability distribution $|\psi(x, t)|^2$. Furthermore, in this case, the time evolution leads to radiation emitted not only by the phonon system but also by the electron, showing that the initial condition is not an exact solution of the continuum system.

We also consider model parameters in the more general setting provided by Eqs. (24)–(28), which were obtained in the variational approach, and start by testing our variational approximation in an extreme case, namely, when both the lattice constant κ and the electron–lattice interactions are large, i.e. $\kappa = 1$ and $\chi = 1$. In Fig. 8 we display the numerical evolution of the coherent stationary state predicted by the variational approximation for those values of the parameters. We observe an asymmetry in the lattice compression ρ_x, which is in contrast to the case of small κ. Once again there are small linear dispersed waves due to the numerical approximation.

To compare with the dynamics in the corresponding full discrete system we inserted the same initial conditions into (6)–(7). Fig. 9 shows that the initial wider wave profile evolves to a thinner one (compare the profiles in Fig. 9(a) and (b)). Another characteristic of the final stationary solutions is that they are in fact breather-like, i.e., the amplitudes of the lattice and electron envelopes oscillate, as Fig. 10 clearly shows. Thus, for these values of the parameters, the time evolution in the continuum system is different from that of the discrete system. In fact, the dynamics in the discrete system bears a strong resemblance to the polarobreather which was found in a slightly different discrete system [18].

5. Concluding remarks

Using a variational approach, we determined the parameter regimes for which mobile, localized, electron states can exist due

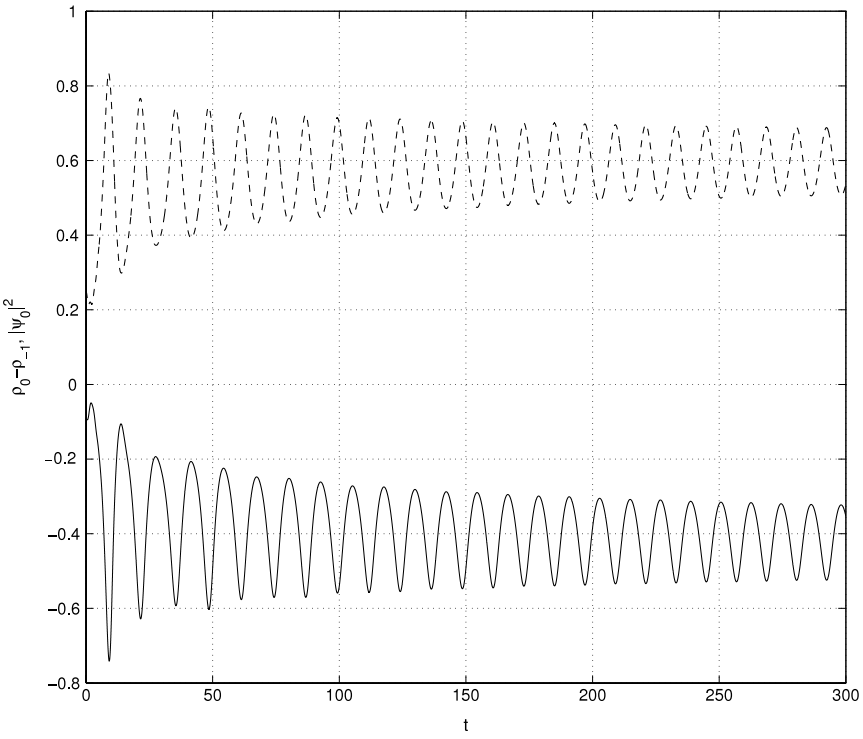

Fig. 10. Evolution of wave amplitudes in Fig. 9. The solid line is for lattice distortion site 0, $\rho_0 - \rho_{-1}$, and the dashed line is for the electron probability density at the same site, $|\psi_0|^2$.

to the influence of dispersive (Debye, inter-site relative motions) and non-dispersive (Einstein, on-site possibly transverse oscillations) phonons. This study complements other reports in which stationary solutions of electron–lattice systems with two types of phonons have been determined [4,5] or in which such systems have been used to describe heat transfer [6–8]. Another related system of equations is that of Zakharov for the study of waves in plasmas [19] and which was the object of analytical investigations in [20–22]. However, while the coupled system of partial differential equations in [20,22] allows for a variational approach based on Gaussian Ansätze or sech pulses for the high frequency and low frequency waves, Eqs. (9)–(10) require exponential Ansätze for the electron wavefunction and for the lattice profiles, as explained in Section 2.1. We have also checked that our variational approach leads to the correct limits when only one type of phonon is considered, namely, the long wave limit investigated here recovers both Davydov's results [1] when only dispersive (Debye) phonons are included and Holstein's [2,3] results when only non-dispersive (Einstein) phonons are considered. Furthermore, we recover the results obtained in [4] for the, pinned, stationary case.

Our main finding is that, when the electron–lattice interaction is dominated by dispersive phonons, localized electron states may only exist for non-zero velocities. Furthermore, for certain values of the lattice parameter κ (see Eq. (8)), the velocity of the traveling electron state must be greater than a given threshold, for that state to be stable. This threshold velocity increases as κ increases. Localized electron states are usually associated with a low mobility. Our results suggest, however, that the picture is a bit more complex since traveling localized states may still lead to high electron mobilities if the electron velocity is sufficiently high.

We have also tested our results by solving the model equations numerically, using as initial conditions the trial functions and wave parameter values found in the variational approximation. In most cases studied, we have found a good agreement between the predictions of the variational approach and the numerical integration of both the continuum and the discrete system. However, when the lattice constant κ and the electron–lattice interaction χ are large, the numerical solutions of the discrete system can be breather-like, something that was not found either in the variational approach or in the numerical integration of the continuum system, suggesting that discreteness is an important factor.

Acknowledgments

The authors wish to express their gratitude to Professors A.P. Chetverikov, W. Ebeling, J.P. Launay and A.A. Minzoni for enlightening discussions. This research has been sponsored by the Mexican grants COFAA-IPN, IPN-CGPI-20150982, Conacyt-177246 and by the Spanish Ministerio of Ciencia e Innovacion under grant MAT2011-26221. LC acknowledges the European Regional Development Fund (ERDF) through the COMPETE—Operational Competitiveness Programme and national funds through FCT Foundation for Science and Technology, under the project PEst-C/MAR/LA0015/2011.

References

[1] A.S. Davydov, Solitons in Molecular Systems, second ed., Reidel, Dordrecht, 1991.
[2] Th. Holstein, Studies of polaron motion: Part I. The molecular crystal model, Ann. Phys. 8 (1959) 325–342.
[3] Th. Holstein, Studies of polaron motion: Part II. The "small" polaron, Ann. Phys. 8 (1959) 343–389.
[4] L. Cruzeiro-Hansson, J.C. Eilbeck, J.L. Marin, F.M. Rusell, Interplay between dispersive and non-dispersive modes in the polaron problem, Phys. Lett. A 266 (2000) 160–166.
[5] Y. Zolotaryuk, J.C. Eilbeck, Analytical approach to the Davydov–Scott theory with on-site potential, Phys. Rev. B 63 (2001) 054302.
[6] E.C. Cuansing, H. Li, J.-S. Wang, Role of the on-site pinning potential in establishing quasi-steady-state conditions of heat transport in finite quantum systems, Phys. Rev. E 86 (2012) 031132.
[7] S. Ma, H. Xu, H. Deng, B. Yang, Phonon transmission and thermal conductance in one-dimensional system with on-site potential disorder, Phys. Lett. A 375 (2011) 1831–1838.

[8] T. Hu, K. Hu, Y. Tang, Anharmonic on-site potential implies asymmetry thermal transport in 1D mass-graded harmonic lattice, Physica B 405 (2010) 4407–4412.
[9] D. Hennig, A.P. Chetverikov, M.G. Velarde, W. Ebeling, Electron capture and transport mediated by lattice solitons, Phys. Rev. E 76 (2007) 046602.
[10] M.G. Velarde, From polaron to solectron: The addition of nonlinear elasticity to quantum mechanics and its possible effect upon electric transport, J. Comput. Appl. Math. 233 (2010) 1432–1445.
[11] L.A. Cisneros-Ake, A.A. Minzoni, Effect of hydrogen bond anharmonicity on supersonic discrete Davydov soliton propagation, Phys. Rev. E 85 (2012) 021925.
[12] M. Christen, P.H. Hünenberger, D. Bakowies, R. Baron, R. Bürgi, D.P. Geerke, T.N. Heinz, M.A. Kastenholz, V. Kärutler, C. Oostenbrink, C. Peter, D. Trzesniak, W.F. van Gunsteren, The GROMOS software for biomolecular simulation: GROMOS05, J. Comput. Chem. 26 (2005) 1719–1751.
[13] D.A. Case, V. Babin, J.T. Berryman, R.M. Betz, Q. Cai, D.S. Cerutti, T.E. Cheatham III, T.A. Darden, R.E. Duke, H. Gohlke, A.W. Goetz, S. Gusarov, N. Homeyer, P. Janowski, J. Kaus, I. Kolossváry, A. Kovalenko, T.S. Lee, S. LeGrand, T. Luchko, R. Luo, B. Madej, K.M. Merz, F. Paesani, D.R. Roe, A. Roitberg, C. Sagui, R. Salomon-Ferrer, G. Seabra, C.L. Simmerling, W. Smith, J. Swails, R.C. Walker, J. Wang, R.M. Wolf, X. Wu, P.A. Kollman, AMBER 14, University of California, San Francisco, 2014.
[14] B.R. Brooks, C.L. Brooks III, A.D. Mackerell Jr., L. Nilsson, R.J. Petrella, B. Roux, Y. Won, G. Archontis, C. Bartels, S. Boresch, A. Caflisch, L. Caves, Q. Cui, A.R. Dinner, M. Feig, S. Fischer, J. Gao, M. Hodoscek, W. Im, K. Kuczera, T. Lazaridis, J. Ma, V. Ovchinnikov, E. Paci, R.W. Pastor, C.B. Post, J.Z. Pu, M. Schaefer, B. Tidor, R.M. Venable, H.L. Woodcock, X. Wu, W. Yang, D.M. York, M. Karplus, CHARMM: The biomolecular simulation program, J. Comput. Chem. 30 (2009) 1545–1614.
[15] A.S. Davydov, A.V. Zolotariuk, Subsonic and supersonic solitons in nonlinear molecular chains, Phys. Scr. 30 (1984) 426–430.
[16] G.B. Whitham, Linear and Nonlinear Waves, Wiley-Interscience, New York, 1999.
[17] L.N. Trefethen, Spectral Methods in Matlab, SIAM, Philadelphia, 2000.
[18] J. Cuevas, P.G. Kevrekidis, D.J. Frantzeskakis, A.R. Bishop, Existence of bound states of a polaron with a breather in soft potentials, Phys. Rev. B 74 (2006) 064304.
[19] V.E. Zakharov, Collapse of Langmuir Waves, Sov. Phys.—JETP 35 (1972) 908–914.
[20] B. Malomed, D. Anderson, M. Lisak, M.L. Quiroga-Teixeiro, L. Stenflo, Dynamics of solitary waves in the Zakharov model equations, Phys. Rev. E 55 (1997) 962–968.
[21] B. Malomed, M.I. Weinstein, Soliton dynamics in the discrete nonlinear Schrödinger equation, Phys. Lett. A 220 (1996) 91–96.
[22] B.S. Ahmed, 1-Soliton solution for Zakharov equations, Adv. Stud. Theor. Phys. 6 (2012) 457–466.